PAPER • OPEN ACCESS

Design optimization of mist cooling for Urban Heat Island mitigation: experimental study on the role of injection density

Design optimization of mist cooling for Urban Heat Island mitigation: experimental study on the role of injection density

G Ulpiani[1,*], E Di Giuseppe[2], C Di Perna[1], M D'Orazio[2] and M Zinzi[3]

[1]Department of Industrial Engineering and Mathematical Sciences, Università Politecnica delle Marche, Via Brecce Bianche, 60131 Ancona, Italy
[2]Department of Construction, Civil Engineering and Architecture, Università Politecnica delle Marche, Via Brecce Bianche, 60131 Ancona, Italy
[3]ENEA, Via Anguillarese 301, 00123 Rome, Ita

[*]giuliaulpiani@gmail.com

Abstract. Climate change, heat waves and weather extremes unveil the need to counteract excess heat and its dramatic consequences on energy, economy, outdoor liveability and, above all, health. In the urban context, further concern arises from the concerted action of cities' materials, fabric, layout, density and activities, which are responsible of heat and pollutants entrapment, of wind force breaking and sweltering microclimates. Ready-to-use, high-impact, smart, cost and energy-effective countermeasures are the only ones having chances to be widely implemented in the short haul. Against this backdrop, this work presents the results obtained from an experimental campaign conducted on a single mitigation technology, meant to reach high local temperature reductions and empowered with climate-adaptive features to be applicable close to any vulnerable target (e.g. schools, hospitals, hospices …): a web of smartly controlled mist sprayers. A prototype was designed and its impacts on the local microclimate were thoroughly characterized. Notably, the nozzle density was investigated to delineate the tradeoffs between evaporative cooling global magnitude and spatial dilution: in fact, by rarefying water emission, a larger air volume can partake to the cooling as it gets harder to reach saturation; conversely the point spatial temperature drop might weaken and become negligible, jeopardizing the whole mitigation strategy. This paper discloses such a controversial point and provides guidelines for the correct design of mist cooling systems for Urban Heat Island counteraction.

1. Introduction

Cities have become complex and dynamic systems of political, economic and bio-physical forces with countless ramifications and interplays between natural and anthropogenic phenomena. Hence, a better understanding of the relations between societies, mass and energy flows is imperative to spot the potential for change to sustainable patterns of consumption and production [1].

A major menace to urban prosperity and livability comes from the joint action of global warming and Urban Heat Island (UHI). UHI is the positive thermal balance of the cityscape compared to the rural surroundings, mostly due to the replacement of natural elements (greenery, water) with asphalt, brick, concrete and dark roofs that act like sponges for heat during the day and warmth emitters overnight. Consequently, urban areas tend to reach dangerous temperatures much faster and much more frequently than rural, less populated landscapes.

Today's climatic upheavals have made the urge for bold UHI counteraction impossible to ignore.
In 2018, unprecedented hot conditions swept through the planet: the temperature touched 43°C in Azerbaijan and stayed over 38°C for a week in Kyoto (Japan). In Norway (Oslo), the mercury hit a +5.9°C above the seasonal mean over a two-week stretch in June, while just a month later, a record-breaking heatwave engulfed Canada (Quebec). Simultaneously, a high of about 48.8°C was recorded inland of Los Angeles. Residents blasted their air conditioners so much they caused power shortages [2]. Ultimately, this means that worldwide we are now divided into well-heeled residents who can afford living in conditioned spaces, and the vulnerable population taking refuge in the outdoors where the exhaust heat of the conditioners is poured. In this vicious cycle, ensuring heat-safe cities and livable outdoors has thus become a priority, not just as a global warming coping mechanism, but as a life saver against extreme weather events, given that such anomalies are envisioned to augment in frequency and amplitude [3][4].

What mostly hinders large-scale interventions is not the scarcity of effective solutions, yet their economic burden. UHI mitigation calls for sophisticated on-site measurements and substantial urban remodeling, both of which are costly, time-consuming and rather invasive. Additionally, for some technologies (e.g. cool materials) ageing issues represent a strong disincentive to extensive applications [5][6].

This study is part of a wider intention to get through the economic and political hold-ups on coping with climate change, by proposing cost-effective, efficient and easily implementable solutions and providing experimentally substantiated design guidelines.
Among the many mitigation technologies at mature state, we elected to investigate direct evaporative cooling by overhead nebulizers.

When a fine water spray is injected by pressurized nozzles it induces absorption of latent heat from the surrounding moist air. Heat and mass transfer mechanisms are thoroughly described in the works by Kachhwaha [7][8] and Sureshkumar [9][10][11]. The potential applications in urban planning and street landscaping (with the purpose of cooling the ambient air) are countless and particularly efficient since the cool medium is close to the individuals: reportedly, the air could be cooled down by 7-10°C (ambient temperature of 30°C and 42°C respectively) [12], as further supported by simulation-based studies [13][14]. From a geographic perspective, spray cooling implementation is well suited for warm, temperate and humid climates, notably the humid subtropical (Cfa) and the hot-summer Mediterranean (Csa). The interest is also growing in Cfb contexts (mild winters and moderately warm summers) as a means to cope with the escalating frequency of weather extremes.
Notwithstanding the cooling performance, water spray was also chosen for the following reasons:

- the cloud of droplets exerts a variety of sanitizing effects on the surroundings: beyond reducing the temperature, it expels dust and scavenges pollutants [15], repels mosquitos and other insects [16][17], attenuates solar radiation, including the UV range responsible of erythema [18];
- as based on evaporative processes, its cooling action gets emphasized at higher dry bulb temperatures (and equal specific humidity) which comes in handy under heat wave emergency;
- overhead systems 1) consume modest quantities of water, thus public fountains and similar might supply sufficient flow; 2) are light and compact thus they can be suspended without subtracting any walkable public land which facilitates bureaucracy.
- No design guidelines exist in literature, despite the wide use to create pedestrian cool spots [19–29]. Yet, harmonizing the cooling action of multiple fine droplets injections is no trivial matter. It entails proper selection and setting of:
- nozzle geometry: according to Farnham et al. [27], single-nozzle nebulizers with Sauter mean diameter between 41 and 45μm could provide non-wetting or nearly non-wetting cooling, without significant performance loss due to the tiny size as also demonstrated by Yoon and Yamada [30]. Accordingly, we selected hollow-cone micro-nebulizers with diameter distribution centred around 10μm. In this case, thermal balance with the surrounding air occurs

within approximately 8mm of the orifice [31] causing negligible net cooling loss because of the initial sensible heat transfer;

- water pressure: the use of constant pressure pumps is recommended to cope with dirt, limestone, dust and corrosion agents that could easily occlude the orifices and alter the cooling performance. High pressure systems are preferred as the cooling efficacy gets enhanced [32]. Consequently, we selected a 70-bar self-compensating pump.

- Injections height: the relative distance between nozzle and user determines the potential for wetting and the cooling magnitude users may experience. We investigated the best setup in [33] by harmonizing environmental measurements and personal feedbacks via statistical tests, regressions and data mining algorithms. Among other results, we estimated the optimal height within 1.2 and 1.5m of users's head.

- Pump control logic: water spray boasts a huge potential for local cooling (up to -10°C [34]). Such a strong action might turn counterproductive in case of temperate climates. In another previous study [35], we demonstrated the ability of fuzzy logic to tweak the water injection to track thermal neutrality. The logic pondered the cooling action based on all the major environmental drivers for evaporative cooling (temperature, relative humidity, wind and solar radiation). It was found to consume up to nearly 70% less than a standard temporized on-off.

- Nozzle density: in multi-nozzle systems another key player is the relative distance between the injections. A plurality of physical processes occurs in their mutual interaction, namely stochastic collisions, coalescence and break-up (also considering secondary impacts among child particles).

- In this context, defining the optimal nozzle density was the objective of this work, so as to provide a comprehensive design guideline. In the following paragraphs materials and methods are described before discussing the experimental results.

2. Materials and methods

The prototype consisted of a high pressure pump (70bar, 919W), a polypropylene filter and about 50m of polyammide tube, arranged in 4 parallel strings, about 1m away from each other and suspended approximately 3m above the ground (see Figure 1). Each line accommodated 6, 1-m spaced nozzles (thus 24 in total) and could be bypassed by closing the corresponding shut-off valve. Each nozzle was secured in place by a couple of clips to fix the jet direction. The water flow absorption was very modest (between 0.7 and 1.5 l/min), thus a simple branch from public fountains provided enough supply. The total cost was less than 1400€. Besides, with extra 200€, the same pump could have supplied 48 nozzles (the double) and cover a surface of nearly 40m^2, with cooling effects further protracted for about 20m from the perimeter and even 3 times more in canyon shaped environments, as substantiated by monitoring data and other existing literature on the topic (e.g. [13]). Thus, the minimum cooled area covered approximately 3,600m^2. The cost for an equal coverage of cool pavements, considering average-efficiency, walkable materials, would have been 16 times more, according to the Italian market [36],not counting the huge infrastructure remodeling costs and the bureaucratic effort.

The pump was controlled and automatically operated via a Virtual Instrument (VI) programmed in LabVIEW to avert unnecessary wear-and-tear and stop in case of rain. The energy consumption was recorded by incorporating a counter that kept track of the activations.

The prototype was assembled on the terrace of the Faculty of Engineering, Università Politecnica delle Marche (Ancona, Italy, 43°35'13.3"N 13°30'54.0"E, 160m a.s.l.). On the top of a hill, this west-oriented open space stays sunny and windy for the most of the summertime in the context of a mild, yet very humid temperate climate (Cfa class according to Köppen and Geiger [37]) with significant rainfall (757mm annual average).

The campaign was conducted over 12 days in July and August, the hottest months of the year. Mist cooling was activated between 10am and 8pm all the days and operated according to the fuzzy logic described in [35]. For 6 days only two rows of nozzles were active (Partial Load, "PL" from now on) 2m distant one from the other. Later, other 6 days were devoted to the full load configuration (termed "FL"), representative of 1m distant strings. Two main groups of sensors were installed to characterize

both the cooled environment and an undisturbed location, to be used as a reference for cooling and humidification calculations. The cooled microclimate was mapped by five miniaturized thermohygrometers (PCMINI52 by Michell Instruments) which come with a response time below 10s and anti-wetting and solar-shielding plastic protections. The five sensors were located right beneath the 4 strings, in the mid-points of the ground-projected perimeter and in the middle of the sprayed area. They were mounted on thin vertical aluminium rods at 1.1.m, to be representative of breast-height for a standing person and head-height for a sitting person (see ISO 7726 [38]).

The undisturbed location was monitored by a meteorological station composed by a thermohygrometer, a tacogonioanemometer and a global radiometer to record the concomitant air temperature, humidity wind and solar radiation about 50m away, on the same terrace. The specs of the sensor network are provided in Table 1.

The sampling rate was 10s to enhance the control logic sensitivity and responsiveness. The analysis was conducted over 1-minute averaged data to mitigate the measurement uncertainty.

Additionally, prior to the monitoring campaign, we test checked the system and performed daily measurements of the water temperature (using a Pt100) to portray the daily swings due to heat transmissions along the pipe.

Table 1. Measured variables and sensors' specifications.

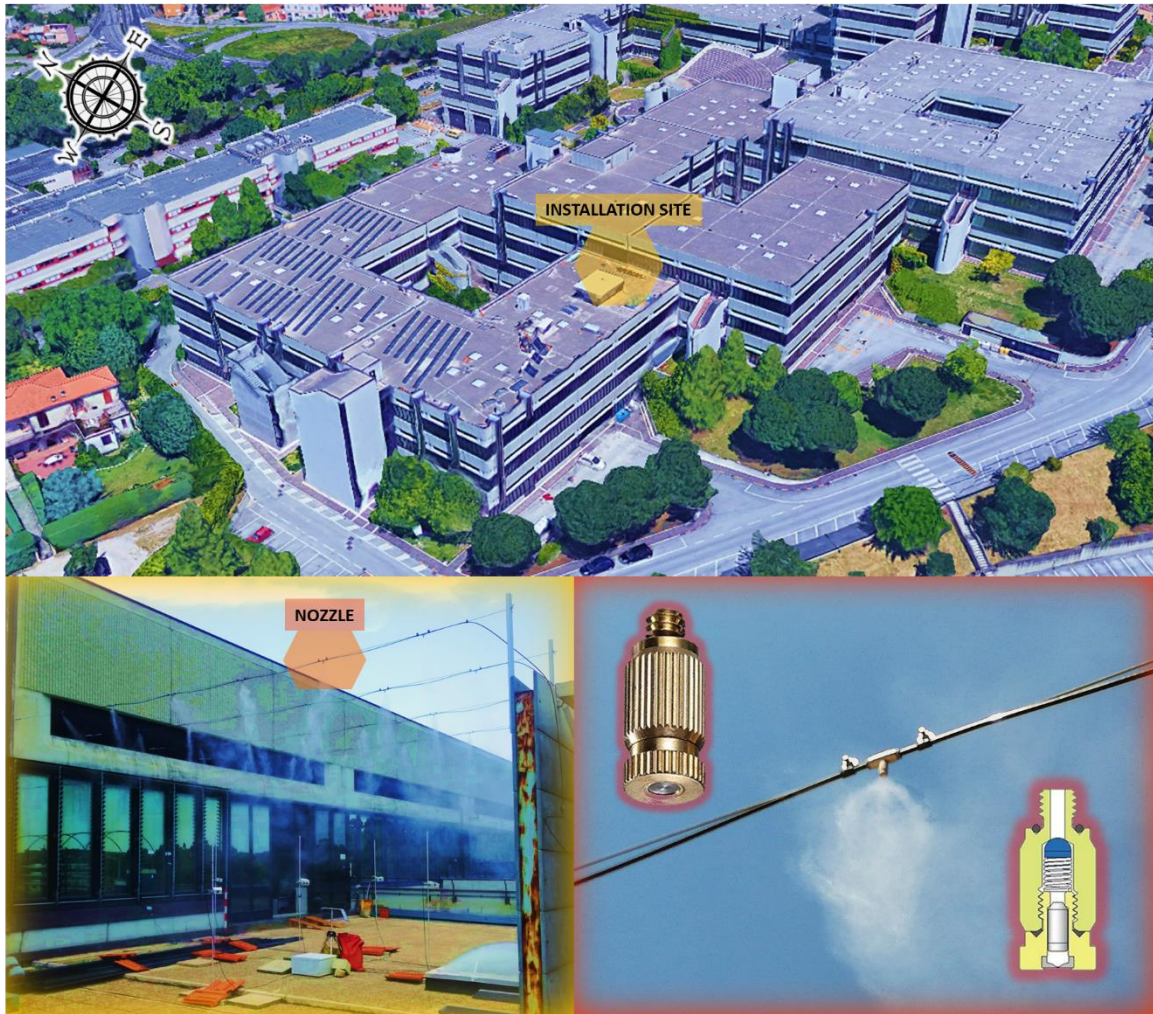| Measure	Sensor type	Height	Range	Accuracy	Responsiveness
			COOLED AREA		
Air temperature + Relative humidity	Mini Thermo hygrometer	1.1m	-20°C÷80°C 0 ÷ 100%	±0.2°C ±2% (10-90%)	T (90%)<10s
			UNDISTURBED AREA		
Air temperature + Relative humidity	Pt100 + capacitive hygrometer	1.7m	-30°C÷70°C 0 ÷ 100%	0.2°C 1.5% (5 ÷ 95%, 23 °C) 2% (<5, >95%, 23 °C)	T (90%)=10s
Wind velocity and direction	Cup Anemometer	2.0m	0 ÷ 60m/s 0 ÷ 360°	1.5% 1	τ(63%)=2.5s τ(63%)=0.7s
Solar radiation	Global Radiometer	1.5m	0 - 2000W/m2	< 5%	T (90%)<30s

Figure 1. Monitoring setting: 3D model of the University terrace on top, the four strings of overhead nebulizers at the left bottom and close-up on a single nozzle at the right bottom (detail and section).

3. Theory and calculations

Nebulization produces a quasi-isoenthalpic adiabatic saturation. If we consider the thermal balance of the evaporating mist as a whole, the governing processes of latent and sensible heat transfer are respectively formalized as follows:

$$Q_{lat} = r \cdot m_e \tag{1}$$
$$Q_{sens} = C_p \cdot m \cdot (t_0 - t_a) \tag{2}$$

Where r is the latent heat of evaporation, taken at $2.45 \cdot 10^6$ J/kg and referred to the mass of evaporating droplets m_e, while C_p is the specific heat capacity of water (thus to be referred to the whole mass m) equal to 4184 J/kg°C. Hence, even in the worst scenario of maximum recorded initial water temperature (36°C) and minimum air temperature accepted by the fuzzy controller (25.2°C), the initial sensible heat loss would have cancelled a negligible 1.85% of the cooling power.

Temperature and humidity beneath the spray were analyzed 1) in time, to quantify the rate of change, spot daily patterns and detect any significant secondary evaporation by comparing the readings over the whole observation window (10am-8pm) and those during the injection; 2) in space, to quantify the zonal variability among the five points of measurement and to quantify the mitigation action against the reference location.

Additionally, to directly compare the two configurations we focused on two days of equal boundary conditions so as to isolate the contribution of the different nozzle density from that of the climatic context. On those days, we computed the evaporative cooling efficiency of the nebulizers in the two configurations, by dividing the daily average cooling by the absorbed electric energy, as follows:

$$\eta = \frac{C_p \cdot m_t \cdot Dt\_avg}{E} \tag{3}$$

where m_t is the total water flow processed over the day and Dt_avg is the daily mean of the temperature difference between the outdoor temperature and the cooler measured point under the spray, calculated considering only the time over which the pump was running.

Finally we addressed the ability of preserving comfortable conditions by tracking comfort neutrality.

4. Results

The focus was first on the recorded temperature drop, as it connotes the technology's mitigation potential. Then we verified that the temperature and humidity variations moderately and evenly distributed beneath the spray. Concomitantly, we looked at energy conservation and comfort preservation.

To identify the two days of equal boundary conditions between PL and FL, we produced Table 2: 30 July and 19 August (bordered rows in the table) differed by less than 0.5°C in terms of mean air temperature, by less than 5% in terms of mean relative humidity, by less than 0.25m/s in terms of wind speed and by less than 100 W/m^2 in terms of solar radiation.

Table 3 summarizes the main statistics on the cooling achieved by the nebulizing system both in partial and full load configuration by comparing the temperature recorded under the spray to that of the meteorological station. We considered the maximum, average and minimum (Dt_max, Dt_min, Dt_avg) among the five measured points. For each, we computed the daily absolute maximum, the 99th and 50th percentiles (median), the inter-quartile range (IQR) and the minimum. The calculation was then repeated only for the time slots of effective pump operation (in bold letters).

The following bullet points recap the main findings:

- on the days of direct comparison (marked by a dashed border in Table 3), the discrepancy between PL and FL was greatly emphasized: interestingly, the difference in terms of maximum and 99th percentile was fairly stable at 2°C, considering Dt_max, Dt_min and Dt_avg as well, while that in terms of median was 1°C lower, yet still constant (notably considering the time slots of actual misting). The IQR was comparable.

- The FL efficiency η was 20.4% versus 16.7% achieved by the PL setup. This is a comprehensive performance parameter, suitable for comparative analysis, since it considers both the hydric and electric consumption.

- Under FL, the absolute maximum touched 7.4°C against 6.4°C reached by PL. Either case, it was recorded on the hottest days, namely the 28th of July for PL and the 13th of August for FL, with daily average temperature of 35.6°C and 32.6°C respectively: this is perfectly in line with previous results [35] and consistent with the underlying physics: indeed, evaporative cooling is more incisive as dry-bulb temperature rises at equal specific humidity, because the higher partial pressure difference boosts the evaporation rate.

- Under PL, negative minimum values were much more frequent and accentuated (+10% occurrences, +24% magnitude compared to FL), meaning that temperatures could be higher beneath the spray than in the surroundings because of severe dilution due to wind entrainment: the chances of coalescence and mutual confinement dropped, depreciating the cooling and deteriorating controllability as well.

- Under PL, no significant inertial processes occurred. Maxima, minima and averages showed no offset between the whole observation window and the times of active misting. Conversely, under FL operation, notably on cloudy and fresher days (refer to the 15th of August), the temperature could further drop by 1.5°C, after the injection ceased. Indeed, coalesced, larger drops from the multiple, closer injections, may have reached the ground and the surfaces all

around, under lower solar radiation and partial pressure difference: this might have introduced significant secondary evaporation. This was especially evident in terms of maxima and 99th percentile; the offset between medians was much less pronounced, meaning that such inertial effects were sporadic.

Table 2. Climatic context during the two monitoring runs. The 14th of August was a rainy day and was thus excluded.

DATE	LOAD	ta [°C]	RH [%]	ws [m/s]	Ioh [W/m²]	E [kWh]	Q [m³]	Dt$_{max}$ [°C]	Dt$_{min}$ [°C]	Dt$_{avg}$ [°C]
25-lug	PL	30,1	61,8	3,1	695,6	3,50	0,16	1,88	0,23	1,12
26-lug	PL	31,4	51,4	2,1	683,3	3,44	0,16	2,72	0,65	1,67
27-lug	PL	29,2	62,1	3,1	696,9	1,59	0,07	1,81	0,13	1,02
28-lug	PL	35,6	48,9	2,2	675,3	4,18	0,20	3,95	0,59	2,08
29-lug	PL	31,0	60,2	2,5	649,8	3,17	0,15	1,98	0,42	1,17
30-lug	PL	30,5	71,3	3,2	671,8	3,46	0,16	1,62	0,24	0,98
13-ago	**FL**	**32,6**	**57,4**	**2,8**	**619,1**	**4,60**	**0,45**	**2,74**	**0,05**	**1,33**
15-ago	**FL**	**29,0**	**59,9**	**2,9**	**525,3**	**1,99**	**0,19**	**2,18**	**0,95**	**1,52**
16-ago	**FL**	**30,0**	**50,8**	**2,2**	**633,0**	**3,11**	**0,30**	**2,29**	**0,38**	**1,36**
17-ago	**FL**	**29,8**	**57,9**	**2,5**	**632,2**	**2,37**	**0,23**	**2,32**	**0,27**	**1,35**
18-ago	**FL**	**29,9**	**66,8**	**2,5**	**621,2**	**2,52**	**0,25**	**2,51**	**0,97**	**1,81**
19-ago	**FL**	**30,2**	**68,7**	**3,3**	**596,8**	**3,35**	**0,33**	**2,57**	**1,36**	**2,01**

Table 3. Daily cooling statistics: PL (on the left) versus FL (on the right).

DAY	LOAD		MAX	99°P	50°P	IQR	MIN	DAY	LOAD		MAX	99°P	50°P	IQR	MIN
25 Jul 2018	PARTIAL	Dt_max	4,03	3,79	2,06	1,10	-0,13	13 Aug 2018	FULL	Dt_max	7,39	6,81	2,76	1,98	-0,20
			4,03	**3,83**	**2,17**	**0,64**	**0,21**				**7,39**	**6,86**	**2,94**	**1,83**	**0,03**
		Dt_min	1,43	1,24	0,68	1,05	-3,11			Dt_min	1,54	1,47	0,55	1,47	-1,37
			1,43	**1,25**	**0,77**	**0,35**	**-1,83**				**1,54**	**1,47**	**0,79**	**1,34**	**-1,24**
		Dt_avg	2,08	2,03	1,44	1,05	-0,77			Dt_avg	2,91	2,71	1,63	1,60	-0,85
			2,08	**2,05**	**1,54**	**0,41**	**-0,31**				**2,91**	**2,74**	**1,81**	**0,90**	**-0,40**
26 Jul 2018	PARTIAL	Dt_max	4,97	4,66	2,92	1,62	0,00	15 Aug 2018	FULL	Dt_max	5,08	4,62	2,41	1,35	-0,34
			4,97	**4,68**	**3,12**	**1,24**	**0,99**				**3,59**	**3,51**	**2,46**	**0,53**	**0,47**
		Dt_min	2,17	2,10	0,99	1,20	-2,76			Dt_min	3,04	2,96	1,10	1,13	-1,62
			2,17	**2,12**	**1,32**	**0,85**	**-2,76**				**1,61**	**1,54**	**1,17**	**0,29**	**-1,43**
		Dt_avg	3,12	3,04	1,86	1,31	-0,45			Dt_avg	3,68	3,50	1,67	0,88	-0,54
			3,12	**3,05**	**2,02**	**0,77**	**0,23**				**2,27**	**2,20**	**1,75**	**0,30**	**0,08**
27 Jul 2018	PARTIAL	Dt_max	3,66	3,43	1,90	1,48	0,17	16 Aug 2018	FULL	Dt_max	4,45	4,27	2,52	1,57	-0,31
			3,08	**3,06**	**2,30**	**0,66**	**0,48**				**4,38**	**4,20**	**2,59**	**0,43**	**1,20**
		Dt_min	1,45	1,37	0,57	1,13	-2,97			Dt_min	1,56	1,45	0,86	1,53	-2,18
			1,45	**1,39**	**0,97**	**0,37**	**-2,31**				**1,56**	**1,49**	**1,19**	**0,33**	**-1,79**
		Dt_avg	2,25	2,17	1,29	1,28	-0,56			Dt_avg	2,57	2,35	1,76	1,17	-0,58
			2,25	**2,20**	**1,70**	**0,40**	**-0,18**				**2,57**	**2,45**	**1,88**	**0,30**	**0,61**
28 Jul 2018	PARTIAL	Dt_max	6,39	6,23	4,25	1,91	0,20	17 Aug 2018	FULL	Dt_max	4,73	4,50	2,63	1,66	-0,29
			6,39	**6,23**	**4,41**	**1,31**	**0,95**				**4,54**	**4,25**	**2,74**	**0,45**	**0,65**
		Dt_min	1,97	1,86	0,96	1,33	-2,98			Dt_min	1,95	1,83	1,10	2,29	-3,97
			1,97	**1,86**	**1,11**	**1,05**	**-2,84**				**1,95**	**1,82**	**1,42**	**0,38**	**-3,67**
		Dt_avg	3,27	3,15	2,40	1,23	-0,02			Dt_avg	2,94	2,62	1,80	1,48	-0,95
			3,27	**3,15**	**2,49**	**0,79**	**0,42**				**2,94**	**2,60**	**2,08**	**0,49**	**-0,78**
29 Jul 2018	PARTIAL	Dt_max	4,06	3,77	2,31	1,61	-0,33	18 Aug 2018	FULL	Dt_max	5,42	5,23	2,79	1,29	0,05
			4,06	**3,82**	**2,47**	**0,65**	**0,33**				**5,42**	**5,21**	**2,98**	**0,35**	**0,39**
		Dt_min	1,42	1,38	0,82	1,42	-2,48			Dt_min	2,53	2,41	1,56	1,87	-2,13
			1,42	**1,40**	**1,01**	**0,38**	**-0,84**				**2,39**	**2,35**	**1,85**	**0,26**	**-1,47**
		Dt_avg	2,23	2,15	1,54	1,27	-0,78			Dt_avg	3,50	3,35	2,22	1,30	-0,29
			2,23	**2,19**	**1,70**	**0,34**	**-0,16**				**3,43**	**3,33**	**2,52**	**0,28**	**0,29**
30 Jul 2018	PARTIAL	Dt_max	3,32	3,11	1,92	1,22	-0,47	19 Aug 2018	FULL	Dt_max	5,35	5,10	2,80	1,25	0,12
			3,32	**3,16**	**1,97**	**0,57**	**-0,13**				**5,35**	**5,15**	**2,97**	**0,72**	**0,89**
		Dt_min	1,42	1,30	0,61	1,14	-2,28			Dt_min	3,46	3,13	1,47	1,18	-1,05
			1,42	**1,30**	**0,73**	**0,54**	**-1,54**				**3,46**	**3,16**	**1,66**	**0,82**	**-0,53**
		Dt_avg	2,14	2,01	1,30	1,16	-0,85			Dt_avg	4,14	3,77	2,22	1,32	-0,10
			2,14	**2,02**	**1,42**	**0,59**	**-0,48**				**4,14**	**3,88**	**2,46**	**0,88**	**0,24**

Table 4 complements the information in Table 3 by looking at the cooling and humidification rate. We computed the 1-minute variation recorded by each probe and derived the maximum, the average and the standard deviation. Maxima were further investigated 1) by looking at when and where the daily absolute occurred, considering also the aggregated water flow given by the antecedent injection duration and 2) by perusing the frequency distribution among the five locations (indicated with the initials of "centre", "north", "south", "west", "east") to spot the most responsive zones at any time of the day.

The most important results are summarized below:

- the maximum temperature drop in a minute time was close to -1°C for both the setups. No repetitive pattern could be associated to the time of the day or to the spraying duration. In contrast, a sharp proclivity to uneven distributions among the five monitored sub-zones emerged under FL operation (much less under PL): the south oriented location was almost always the coolest spot (both in terms of absolute maximum and in terms of daily occurrences), as a result of dominant winds from north-west.
- The maximum humidity increment under FL operation was twice that under PL's (+13.4% versus +7.8%) and frequently occurred late in the afternoon. This unbalance was expected. With over +10% humidity in a minute time, the FL configuration was responsible of temporary hygrometric discomfort: the 70% limit proposed by Ishii et al. [39] was trespassed on all the monitoring days, although for a very limited time frame, peaking at 84% on the 19th of August. On average, the relative humidity beneath the spray was lower than 65%, which is the limit proposed by Dominguez [28]. Deeper investigation of the humidity implications was conducted in [35] on the same setup.
- On the days of direct comparison (bordered in Table 4), the rate of change was pretty much equal.

Table 4. Cooling and humidification rates.

COOLING RATE: $\Delta T-/min$												
					max cooling						**avg**	**standard deviation**
DATE		**[°C]**	**where**	**when**	**spraying duration [s]**	**spatial distribution [% of occurrence]**						
						C	**E**	**S**	**W**	**N**		
25/Jul	PL	-0,69	W	○ 11:28	30	19,72	16,96	23,18	20,07	20,07	-0,17	0,13
26/Jul	PL	-0,89	S	◑ 13:49	70	12,24	15,38	27,62	19,58	25,17	-0,20	0,16
27/Jul	PL	-0,52	W	◔ 14:00	110	16,28	20,93	21,71	24,81	16,28	-0,19	0,13
28/Jul	PL	**-1,07**	S	● 18:31	180	17,35	15,82	24,23	17,09	25,51	-0,21	0,16
29/Jul	PL	-0,66	E	● 18:01	160	19,57	16,30	25,72	16,67	21,74	-0,17	0,12
30/Jul	PL	-0,57	S	◔ 13:34	100	16,44	22,60	24,66	15,41	20,89	-0,15	0,10
13/Aug	FL	**-0,96**	S	○ 12:31	240	13,72	15,21	33,17	17,96	19,95	-0,21	0,15
15/Aug	FL	-0,52	S	◑ 15:01	50	14,37	16,17	33,53	15,57	20,36	-0,17	0,12
16/Aug	FL	-0,72	S	◕ 16:53	60	14,29	13,91	31,20	18,80	21,80	-0,17	0,13
17/Aug	FL	-0,94	S	● 18:12	60	16,13	16,67	27,42	16,13	23,66	-0,17	0,13
18/Aug	FL	-0,40	W	◔ 13:39	80	16,67	13,33	26,67	21,43	21,90	-0,13	0,10
19/Aug	FL	-0,48	S	○ 11:20	30	14,73	13,18	31,78	18,60	21,71	-0,15	0,10
HUMIDIFICATION RATE: $\Delta RH+/min$												
					max humidification						**avg**	

DATE		[%]	where	when	spraying duration [s]	spatial distribution [% of occurrence]						standard deviation
						C	E	S	W	N		
25/Jul	PL	4,16	E	◑ 12:02	190	12,64	18,77	27,80	22,02	18,77	1,03	0,82
26/Jul	PL	6,93	S	○ 10:01	80	10,47	21,66	28,16	23,83	15,88	1,43	1,26
27/Jul	PL	3,53	E	◑ 16:00	30	16,67	15,87	26,19	27,78	13,49	0,97	0,68
28/Jul	PL	**7,78**	N	◑ 16:13	110	9,32	25,75	21,37	22,47	21,10	2,01	1,39
29/Jul	PL	5,97	E	● 17:13	20	14,52	18,55	27,02	23,39	16,53	1,10	0,90
30/Jul	PL	5,10	W	● 17:15	50	8,78	19,85	29,39	19,47	22,52	1,11	0,87
13/Aug	FL	**13,39**	S	◐ 13:37	40	9,09	15,72	30,47	20,88	23,83	3,35	2,24
15/Aug	FL	10,84	S	◔ 12:41	30	5,16	21,29	36,77	19,35	17,42	2,78	2,40
16/Aug	FL	10,58	W	◑ 15:40	170	9,48	16,81	35,34	18,97	19,40	2,58	2,33
17/Aug	FL	11,28	C	● 18:47	50	12,00	16,50	35,50	22,50	13,50	1,89	1,97
18/Aug	FL	8,53	S	◐ 14:44	20	8,05	20,69	35,06	21,84	14,37	1,68	1,53
19/Aug	FL	7,96	E	◑ 15:20	50	5,96	21,10	39,91	16,97	16,06	1,43	1,14

Finally, to complete the comfort assessment we quantified frequency and magnitude of deviation from the neutral temperature, namely the temperature at which people claim to feel neither cool nor warm on average [40]. It coincides with the central thermal sensation in the ASHRAE 7-point scale. In our study, the neutral temperature was set at 27.2°C according to a transveral survey conducted in Rome [41]. To verify which configuration closely tracked the comfort zone, we binned the offset from thermal neutrality into progressively larger bands and plotted for each of them the number of occurrences (Figure 2). We compared the 30 July and 19 August measurements. FL blatantly outperformed PL: it guaranteed an almost perfect tracking of comfortable conditions by keeping the offset at less than 1°C for the 37% of the time (against only 8% under PL) and over 3°C for about the 12% of the time (against the 73% under PL).
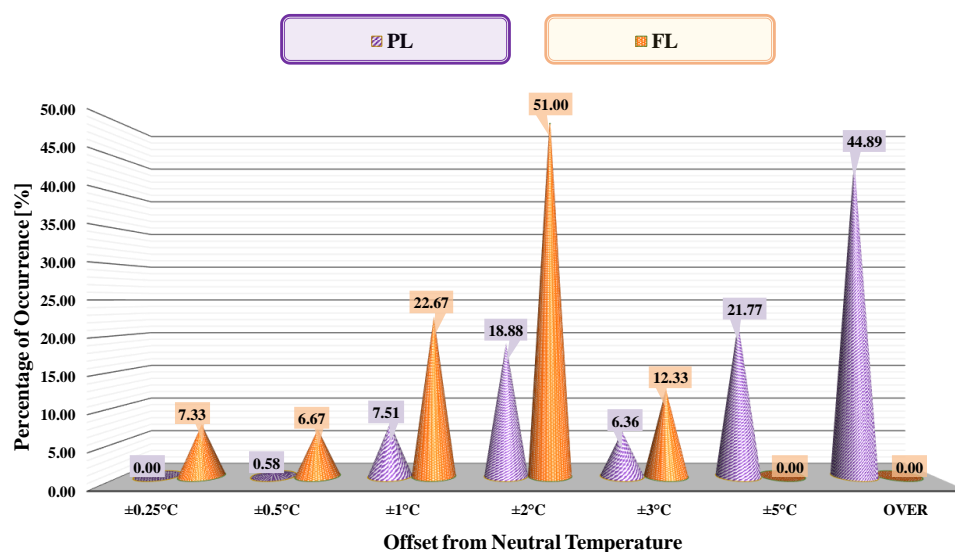

Figure 2. Frequency distributions of Dt_neutral in progressively larger bands.

5. Conclusions

An experimental study was conducted to investigate how nozzle density affects the cooling and humidification profiles of overhead misting systems used to mitigated potential outdoor overheating. The prototype consisted of 24, 1m-interspaced nozzles arranged in 4 rows at about 3m above ground level and served by a high-pressure, self-compensating pump. Each branch was fit with a shut-off valve: in this way we could monitor both full load conditions (FL) and partial load conditions (PL with only two active branches, at about 2m one from the other). The campaign took place in the context of a very humid and rainy temperate climate over 12 days of the hottest months. Mist cooling was activated between 10am-8pm and operated according to the fuzzy logic described in [35].

We concluded that FL was the best option by far, given that:

- the cooling capacity was enhanced (FL's maximum of 7.4°C against PL's maximum of 6.4°C) going 2°C further down than PL under equal boundary conditions;
- PL was much more susceptive to wind entrainment. The cooling was thus ineffective on a much higher number of occasions, deteriorating controllability as well;
- under partial load, no significant inertial processes intervened. Secondary evaporation basically never reinforced the mitigation action;
- the efficiency η was 20.4% versus 16.7% achieved by the PL setup, considering both hydric and electric consumptions;
- FL guaranteed an almost perfect tracking of comfortable conditions by keeping the offset at less than 1°C for the 37% of the time (against only 8% under PL) and over 3°C for about the 12% of the time (against the 73% under PL).

On the other hand, FL favored uneven spatial distributions and greater humidity incremental rates. Borrowing from previous studies too, the authors conclusively suggest that a 1-m dense web of nebulizers suspended at about 1.5m from people's head and fuzzy controlled might truly come in handy against outdoor overheating, notably in urban contexts and under heat wave emergency. This results were experimentally substantiated for Cfa climate. Further investigation might be appropriate to extend their validity to other contexts.

References

[1]   Broto V C, Allen A, Rapoport E, 2012 Interdisciplinary Perspectives on Urban Metabolism. *Journal of industrial ecology.* Available at: doi:10.1111/j.1530-9290.2012.00556.x.

[2]   Fleming A, Michaelson R, Youssef A, Holmes A, Fonbuena C, Robertson H 2018 Heat: the next big inequality issue. *Guard.* [Online] available: https://www.theguardian.com/cities/2018/aug/13/heat-next-big-inequality-issue-heatwaves-world

[3]   IPCC, 2018. *Fifth Assessment Report (*AR5)

[4]   Abadie L M, Chiabai A, Neumann M B 2019 Stochastic diffusion models to describe the evolution of annual heatwave statistics: A three-factor model with risk calculations. *Science of the Total Environnment* **646** 670–684. Available at: doi:10.1016/j.scitotenv.2018.07.158.

[5]   Tsoka S, Theodosiou T, Tsikaloudaki K, Flourentzou F 2018 Modeling the performance of cool pavements and the effect of their aging on outdoor surface and air temperatures. S*ustainable Cities and Society* **42** 276–288. Available at: doi:10.1016/j.scs.2018.07.016.

[6]   Paolini R, Zinzi M, Poli T, Carnielo E, Mainini A G 2014 Effect of ageing on solar spectral reflectance of roofing membranes: Natural exposure in Roma and Milano and the impact on the energy needs of commercial buildings. *Energy and Buildings* **84** 333–343. Available at : doi:10.1016/j.enbuild.2014.08.008.

[7]   Kachhwaha S S, Dhar P L, Kales S R 1998 Experimental studies and numerical simulation of evaporative cooling of air with a Horizontal parallel flow. *International Journal of Heat and Mass Transfer.*

[8]   Kachhwaha S S, Dhar P L, Kale S R 1998 Experimental studies and numerical simulation of evaporative cooling of air with a water spray - II. Horizontal counter flow. *International Journal of Heat and Mass Transfer* **41** 465–474. Available at: doi:10.1016/S0017-

9310(97)00131-2.

[9]   Sureshkumar R, Kale S R, Dhar P L 2008 Heat and mass transfer processes between a water spray and ambient air – I . Experimental data. *Applied Thermal Engineering* **28** 349–360. Available at: doi:10.1016/j.applthermaleng.2007.09.010.

[10]   Sureshkumar R, Kale S R, Dhar P L 2008 Heat and mass transfer processes between a water spray and ambient air - II. Simulations. *Applied Thermal Engineering* **28** 361–371. Available at: doi:10.1016/j.applthermaleng.2007.09.015.

[11]   Sureshkumar R, Kale S R, Dhar P L 2007 Effects of spray modeling on heat and mass transfer in air-water spray systems in parallel flow. *International Communications in Heat and Mass Transfer* **34** 878–886. Available at: doi:10.1016/j.icheatmasstransfer.2007.03.001.

[12]   F.J.S. Dominguez, S. Alvarez, de la Flor 2016 The effect of evaporative techniques on reducing urban heat ed Santamouris M, Kolokotsa D *Urban Clim. Mitig. Tech.* (Routledge, London)

[13]   Chatzidimitriou A, Liveris P, Bruse M, Topli L 2013 Urban Redevelopment and Microclimate Improvement : A Design Project in Thessaloniki , Greece. *PLEA 2013 Sustain. Archit. a Renew. Futur.*

[14]   Nunes J, Zoilo I, Jacinto N, Nunes A, Campos T, Pacheco M, Fonseca D 2016 Misting-cooling systems for microclimatic control in public space. [Online] available: http//Www.Proap.Pt/847/Misting-Cooling-Systemsfor- Microclim.

[15]   Pruppacher H R, Klett J D 1997 *Microphysics of Clouds and Precipitation*

[16]   Boston T W 2006 *Device for eliminating mosquitos*

[17]   Anzivino A 2003 *Water-spray apparatus for repelling and deterring birds*

[18]   Dombrovsky L A, Solovjov V P, Webb B W 2011 Attenuation of solar radiation by a water mist from the ultraviolet to the infrared range. *Journal of Quantitative Spectroscopy and Radiative Transfer* **112** 1182–1190. Available at: doi:10.1016/j.jqsrt.2010.08.018.

[19]   Martins T A L, Adolphe L, Bonhomme M, Bonneaud F, Faraut S, Ginestet S, Michel C, Guyard W 2016 Impact of Urban Cool Island measures on outdoor climate and pedestrian comfort: Simulations for a new district of Toulouse, France. S*ustainable Cities and Society* **26** 9–26. Available at: doi:10.1016/J.SCS.2016.05.003.

[20]   Chen L, Wen Y, Zhang L, Xiang W N 2015 Studies of thermal comfort and space use in an urban park square in cool and cold seasons in Shanghai, *Building and Environment* **94** 644–653. Available at: doi:10.1016/j.buildenv.2015.10.020.

[21]   Wang Y, De Groot R, Bakker F, Wörtche H, Leemans R 2017 Thermal comfort in urban green spaces: a survey on a Dutch university campus. *International Journal of Biometeorology* **61** 87–101. Available at: doi:10.1007/s00484-016-1193-0.

[22]   Narumi D, Shigematsu K, Shimoda Y 2009 Effect of the Evaporative Cooling Techniques by Spraying Mist Water on Reducing Urban Heat Flux and Saving Energy in Apartment House. *2nd Int. Conf. Countermeas. to Urban Heat Islands* **7** 175–181.

[23]   Nishimura N, Nomura T, Iyota H, Kimoto S 1998 Novel water facilities for creation of comfortable urban micrometeorology, *Sol. Energy* **64** 197–207. Available at: doi:10.1016/S0038-092X(98)00116-9.

[24]   O'Malley C, Piroozfar P, Farr E R P, Pomponi F 2015 Urban Heat Island (UHI) mitigating strategies: A case-based comparative analysis. S*ustainable Cities and Society* **19** 222–235. Available at: doi:10.1016/J.SCS.2015.05.009.

[25]   Manteghi G, Bin Limit H, Remaz D 2015 Water Bodies an Urban Microclimate: A Review. *Mathematical Models and Methods in Applied Sciences* **9** 1. Available at: doi:10.5539/mas.v9n6p1.

[26]   Montazeri H, Toparlar Y, Blocken B, Hensen J L M 2017 Simulating the cooling effects of water spray systems in urban landscapes: A computational fluid dynamics study in Rotterdam, The Netherlands. *Landscape and Urban Planning* **159** 85–100. Available at: doi:10.1016/j.landurbplan.2016.10.001.

[27]   Farnham C, Nakao M, Nishioka M, Nabeshima M, Mizuno T 2011 Study of mist-cooling for semi-enclosed spaces in Osaka, Japan. *Procedia Environmental Science* **4** 228–238.

Available at: doi:10.1016/j.proenv.2011.03.027.

[28] Dominguez S A , De La Flor F J S 2016 The effect of evaporative techniques on reducing urban heat ed Santamouris M, Kolokotsa D *Urban Clim. Mitig. Tech.* (Routledge, London)

[29] Wang J, Meng Q, Tan K, Zhang L, Zhang Y 2018 Experimental investigation on the influence of evaporative cooling of permeable pavements on outdoor thermal environment. *Building and Environment* **140** 184–193. Available at: doi:10.1016/j.buildenv.2018.05.033.

[30] Yoon G, Yamada H, Okumiya M 2008 Study on a cooling system using water mist sprayers; system control considering outdoor environment. *Symposium on Human-Environment System* (Cheju, Korea), p. 4.

[31] Holterman H J 2003 Kinetics and evaporation of water drops in air (Wageningen: Wageningen University and research)

[32] Huang C, Ye D, Zhao H, Liang T, Lin Z, Yin H, Yang Y 2011 The research and application of spray cooling technology in Shanghai Expo. *Applied Thermal Engineering* **31** 3726–3735. Available at: doi:10.1016/j.applthermaleng.2011.03.039.

[33] Ulpiani G, Di Giuseppe E, Di Perna C, D'Orazio M, Zinzi M 2019 Thermal comfort improvement in urban spaces with water spray systems: Field measurements and survey. *Building and Environment* **156** 46–61. Available at: doi:https://doi.org/10.1016/j.buildenv.2019.04.007.

[34] Santamouris M, Ding L, Fiorito F, Oldfield P, Osmond P, Paolini R, Prasad D, Synnefa A 2017 Passive and active cooling for the outdoor built environment – Analysis and assessment of the cooling potential of mitigation technologies using performance data from 220 large scale projects. *Sol. Energy* **154** 14–33. Available at: doi:10.1016/j.solener.2016.12.006.

[35] Ulpiani G, Di Perna C, Zinzi M 2019 Water nebulization to counteract urban overheating: Development and experimental test of a smart logic to maximize energy efficiency and outdoor environmental quality. *Appl. Energy* **239** 1091–1113. Available at: doi:10.1016/j.apenergy.2019.01.231.

[36] Diasen Srl 2018 *Annual Market Cost Analysis on Cool Materials*, Confidential.

[37] Köppen W, Geiger R 1936 Das Geographische System der Klimate. *Handb. Der Klimatologie.*

[38] ISO, 1998. ISO 7726:1998 Ergonomics of the thermal environment -- Instruments for measuring physical quantities.

[39] Ishii T, Tsujimoto M, Yoon G, Okumiya M 2009 Cooling System with Water Mist Sprayers for Mitigation of Heat-island Drymist system. *Seventh Int. Conf. Urban Clim.* (Yokohama, Japan), 2–3

[40] Fanger P O 1972 *Thermal comfort, analysis and application in environmental engineering* New York, McGrew-Hill.

[41] Salata F, Golasi I, De Lieto Vollaro R, De Lieto Vollaro A 2016 Outdoor thermal comfort in the Mediterranean area. A transversal study in Rome, Italy. *Build. Environ.* **96** 46–61. Available at: doi:10.1016/j.buildenv.2015.11.023.